Finite Element Modelling of Hot Extrusion of TI-6AL-4V Alloy

Maziar Ramezani, Thomas Neitzert

Department of Mechanical Engineering, Auckland University of Technology, Auckland, New Zealand.

Abstract— *A finite element (FE) model is developed in this paper for simulating the direct extrusion process of Ti-6Al-4V alloy under isothermal condition. The model takes into account the heat generation due to plastic deformation of the billet as well as the frictional heat in the billet-tool interface. A series of simulations have been conducted to investigate the effect of key process parameters on stress and strain distribution, maximum ram speed and maximum pressure applied to the die. The FE model has been compared with a theoretical model and the results show good correlation in terms of predicting ram load. The developed FE model can be used for investigating direct extrusion and selecting appropriate die design parameters for the process.*

Keywords—Die design, FE simulation, hot extrusion, Ti-6Al-4V.

I. INTRODUCTION

Titanium alloys are extensively used in different applications such as aerospace, pressure vessels, turbine blades, and surgical implants because they possess high strength-to-weight ratio and excellent corrosion resistance. The two-phase Ti–6Al–4V alloy displays an optimal combination of mechanical properties and workability which makes it one of the most widely used titanium alloys (Enayati et al., 2011). The raw-material cost of this alloy can be compensated for by adopting economical forming routes. Recently, considerable interest has been shown in the manufacture of titanium components by extrusion techniques, which can lead to efficient utilisation and conservation of these expensive alloys (Cai et al., 2013). The direct extrusion of titanium and its alloys generally demands a high magnitude of forming stresses. These stresses are likely to be accentuated while extruding certain titanium alloys with higher flow stresses and may necessitate the use of expensive carbide punches for the process (Srinivasan and Venugopal, 1999). The technical conditions which determine the extrusion quality include extrusion ratio, die profile and frictional condition at the tool/workpiece interface (Wang et al., 2012). Optimization of these parameters is always an important task for design engineers in the manufacturing industry (Ramezani and Neitzert, 2016).

Direct extrusion process is considered for this research as illustrated in Fig. 1. In this process, the ram applies force to the dummy block, transmitting the force to the billet. Initially, this force causes upset—the whole billet is deformed to fit the container shape and there is initial flow further into the die. After upsetting, the extrusion process takes place, producing the desired extrudate. The metal for the extrudate comes from the deformation zone within the billet. During the entire process, the material flow and shape of the deformation and any dead metal zones are evolving. After most of the billet has been extruded, the flow can contort to such a degree that extrusion is no longer feasible (Tibbetts and Wen, 1998). The remainder of the billet is removed and the entire process is repeated. The design of the extrusion process will be time- and cost consuming if it relies on trial and error. The finite element method (FEM) can be used to simulate the process, to shorten the development cycle and to improve the extrusion technology. In this paper, the finite element simulation was employed to investigate the distribution of strain, temperature and effective stress during direct extrusion of Ti-6Al-4V alloy under different design and processing conditions. Until now, the extrusion technology of certain materials, such as aluminum and copper alloys has made a great improvement through the wide application of FEM method (Kim et al., 2001). For the extrusion of titanium alloys, the FEM has also begun to attract the attention of researchers and a few studies have been done (see e.g. Si et al., 2011; Liu et al., 2013). But those works mainly focused on the heat transfer of the billet and there is no systematic research available in literature to investigate the effect of key process parameters on direct extrusion of Ti–6Al–4V alloy.

The main objective of this investigation is to study the direct extrusion behavior of Ti–6Al–4V titanium alloy in direct extrusion and to study the effect of key process parameters on stress and strain distribution, maximum ram speed and maximum pressure applied

to the die. A commercial FEM code, ABAQUS V.12, was used to describe the deformation behavior of Ti–6Al–4V alloy during its axisymmetric extrusion through a conical die as a function of ram speed, die fillet radius, die angle and coefficient of friction.

II. FINITE ELEMENT SIMULATION

In the finite element model, the billet and the container form the main components. In the model definition in ABAQUS/Standard, the container is defined by rigid surfaces and the billet is a deformable part. The process is displacement controlled and instead of modeling the ram, the corresponding displacement is applied on the top of the billet. CAX4RT elements are used to mesh the billet. CAX4RT is a 4-node thermally coupled axisymmetric quadrilateral, bilinear displacement and temperature, reduced integration, hourglass control element. Due to the axisymmetry of the process, only 2-D meshes of the container and billet are generated (Ramezani and Neitzert, 2016).

The billet used in the axisymmetric extrusion simulation has a length of L_0=58*mm* and a radius of D_0=58*mm* (see Fig. 2). The billet goes through a die with an opening radius of D_i=20 and the fillet radius (R_1) and the angle of the container (α) will change to investigate their effects on the process. Fig. 3 shows the FE mesh of the extrusion process at the beginning and end of loading. The analysis of the extrusion process is based on consideration of the coupled temperature-displacement condition.

The simulation begins with the billet in contact with the container. The displacement representing the ram movement will then be applied at the top of the billet. The interface between the container and the billet is modeled using an automatic surface to surface contact algorithm. Throughout the simulation, nodes on the center line of the billet are fixed in all direction to prevent any rigid body motion of the billet, which may result in numerical errors during the simulation.

One of the major requirements for computer simulations is the incorporation of material properties through realistic models. The billet material undergoes large strain plastic deformation and therefore true stress–true strain test data up to fracture are required in order to define the suitable sheet material model in the simulations. The billet material is Ti–6Al–4V alloy and the container is made of H13 tool steel. The necessary mechanical and thermal properties of billet material for simulations were obtained from Momeni and Abbasi (2010) and Roy and Suwas (2013). The present analysis assumes a constant friction coefficient between the billet and the tool under isothermal condition. The model also takes into account the heat generation during the extrusion process through the shape variation as well as the frictional work done on the die walls. The velocity of the ram and the coefficient of friction are other factors changing during analyses. The present numerical analysis has investigated the stress and strain distribution, the contact pressure on the container and the ram load during the extrusion process.

III.RESULTS AND DISCUSSIONS

Figure 4 depicts different stages of direct extrusion simulation. The process starts with applying pressure on the top of the billet and this pressure develops throughout the billet causing upsetting and the whole billet will deform to fit the container and start the initial material flow around the corner of the die. After upsetting, the billet is forced to fill the die outlet and then the extrusion process takes place and the billet deforms drastically and goes through the die causing permanent plastic deformation and cross section change.

Fig. 5 shows the distribution of plastic strain and principal stress in the Y direction at the end of the process. It can be seen that as the material flows and extrudes through the die orifice, the state of stress and strain changes. The upper section of the billet is under significant compressive stress and strain condition, while the part of the material which is already extruded experiences lower level tensile stress and strain state. Fig. 6 shows the distribution of the contact pressure on the die at the last stage of the simulation for α=25°, R_1=15mm and R_2=10mm. It can be seen that the maximum pressure is 4.2GPa and occurs immediately after the first bend in the container. Based on the results, the contact pressure on the container wall is quite significant and this pressure eases after the die opening. This contact pressure can be considered as an important factor for estimating the die life. Die material usually starts cracking at the location of maximum contact pressure if it is not strong enough to withstand the predicted pressure level.

The variation of the extrusion force under extrusion conditions of α=25°, μ=0.1, R_1=15mm and R_2=10mm is plotted in Fig. 7. The extrusion load curve can be divided into three stages: start of material flow, filling the die outlet and the final extrusion stage. At the initial stage of the extrusion, when contacting the die, the billet starts plastic deformation around the corners of the die angle. At this stage, the extrusion load initially increases to about 5 kN. The material continues to flow until the die is completely filled by the billet and the extrusion process starts. At this stage

the extrusion load increases immediately to about 25 kN. At the last step which is the extrusion steady-stage, the billet continuously passes through the outlet of the die and the extrusion load remains relatively stable.

To validate the results of FE simulations, the predicted extrusion load curve will be compared with the results of theoretical model. In the direct extrusion process, the total extrusion load can be expressed as:

$$F_{total} = f_c + f_d + F_d \qquad (1)$$

where F_{total} is the total extrusion load, f_c is the friction force between billet and container wall, f_d is friction force between extrudate and die bearing, and F_d is the force required for the plastic deformation of billet material, and it is a function of total strain, strain rate and temperature. Tiernan et al. (2005) proposed the following equation for predicting the extrusion load:

$$F_{total} = 2k_f \left[4\mu \left(\frac{H}{D} + \frac{h}{d} \right) + \left(\frac{\mu}{\sin(90-\alpha)} + 1 \right) \ln \frac{D^2}{d^2} \right] \times \frac{\pi D^2}{4} \qquad (2)$$

where μ is the coefficient of friction at die/billet interface, D the billet diameter (mm); d the die land diameter (mm), h the die land height (mm), α the die angle (◦), H the billet height (mm) and k_f is the maximum tangential stress at die–billet interface (N/mm^2). The extrusion load obtained from Eq. (2) is plotted in Fig. 7 and as can be seen in the figure, it shows good correlation with the results of the FE simulation. In general, the FE model tends to predict a slightly lower ram load compared to the theoretical model. This gives us confidence that the FE model developed in this paper is accurate and we continue with our FE analysis.

The effect of ram speed on maximum extrusion load and maximum contact pressure are shown in Figs. 8 and 9. The ram speed varies from 8mm/s to 48mm/s. It can be seen that at higher ram speeds, the ram force decreases, while the contact pressure increases, however; these changes are not remarkable. Figs. 10 and 11 show the effect of die angle (α) on maximum extrusion load and maximum contact pressure. It can be seen that after an increase in ram load for α=35°, the maximum ram load decreases constantly by increasing the die angle. This is mainly due to better material flow in the container at higher angles. The die angle of α=35° seems to be the critical angle in terms of material flow and should be avoided in the die design for the type of material and the billet dimension studied here. It can be seen from Fig. 11 that maximum contact pressures at α=15° and α=35° are slightly higher which again can be due to the difficulties in flow of material to the die opening at these angles. α=25° is an appropriate choice for the die design in terms of minimizing both ram load and contact pressure.

As illustrated in Figs. 12 and 13, the coefficient of friction has a quite significant effect on maximum extrusion load and maximum contact pressure. Generally, as the coefficient of friction increases, the ram force and the contact pressure on the die surface increase. This is mainly due to the severity of contact conditions that affect the flow of the billet material to the die. Based on the figures, the variation of maximum ram force versus friction coefficient is close to linear. However, the variation of maximum contact pressure versus friction coefficient can be fitted by an exponential function. It is worth pointing out that the FE model developed in this paper considers the temperature rise in the deformation zone due to adiabatic and frictional heating and the increase in temperature due to a higher coefficient of friction helps the material to flow better toward the die orifice, however this is not enough to overcome the decelerating condition at higher friction coefficients and overall, the higher coefficient of friction has an adverse effect on the extrusion process of Ti–6Al–4V alloy.

The effect of die fillet radius R_1 on maximum extrusion load and maximum contact pressure are shown in Figs. 14 and 15, while R_2 is considered to be constant. The fillet radius R_1 varies from 5mm to 20mm. Based on Figure 14, the maximum ram force decreases slightly with increase in fillet radius and then becomes constant after R_1=15mm and the same trend is observed for the maximum contact pressure. The slight decreases are mainly due to the fact that bigger fillets assist the flow of the material around the die corner and a slightly lower force is required to push the material out of the die.

IV. CONCLUSIONS

The direct extrusion process simulations of Ti–6Al–4V alloy were performed using ABAQUS software. Despite the broad application of extrusion process in the titanium industry, the design of the tools and the selection of the die materials are still usually based on trial and error efforts, a very expensive and time consuming procedure. The proposed model can be used in industrial applications to create reliable finite element simulations for describing the extrusion

process, optimizing the tool design and predicting defects in the process. This will be of great help to industries in reducing trial and error efforts during the pre-production phase of a product and quality control during production. The effects of ram speed, die fillet radius, die angle and coefficient of friction on the process have been investigated and the results can be used for selecting appropriate die design parameters for the extrusion process.

REFERENCES

[1] Cai, H.-J., Ye, W.-J., Hui, S.-X., Liu, R. (2013) Effects of hot extrusion on the microstructure and properties of Ti-6Al-4V titanium alloy. *Beijing Keji Daxue Xuebao/Journal of University of Science and Technology Beijing* 35 (7) , pp. 895-900.

[2] Enayati, S., Mousavi, S.A.A.A., Mohammad Ebrahimi, S., Belbasi, M., Sultan Bayazidi, M. (2011) Effects of temperature and effective strain on the flow behavior of Ti6Al4V. *Journal of the Franklin Institute* 348 (10) , pp. 2813-2822.

[3] Kim, N.H., Kang, C.G., Kim, B.M. (2001) Die design optimization for axisymmetric hot extrusion of metal matrix composites. *International Journal of Mechanical Sciences* 43 (6) , pp. 1507-1520.

[4] Liu, R., Wang, Z., Liu, D., Bai, C., Cui, Y., Yang, R. (2013) Microstructure and tensile properties of Ti-45.5Al-2Cr-2Nb-0.15B alloy processed by hot extrusion. *Jinshu Xuebao/Acta Metallurgica Sinica* 49 (6) , pp. 641-648.

[5] Momeni, A., Abbasi, S.M. (2010) Effect of hot working on flow behavior of Ti-6Al-4V alloy in single phase and two phase regions. *Materials and Design* 31 (8) , pp. 3599-3604.

[6] Ramezani, M., Neitzert, T. (2016) Computer simulations of direct extrusion of sintered Ti-6Al-4V alloy at elevated temperature. *International Journal of Applied Engineering Research* 11 (6) , pp. 3848-3852.

[7] Roy, S., Suwas, S. (2013) The influence of temperature and strain rate on the deformation response and microstructural evolution during hot compression of a titanium alloy Ti-6Al-4V-0.1B. *Journal of Alloys and Compounds* 548 , pp. 110-125.

[8] Si, J., Gao, F., Han, P., Zhang, J. (2011) Simulation on extrusion process of TiAl alloy. *Intermetallics* 19 (2) , pp. 169-174.

[9] Srinivasan, K., Venugopal, P. (1999) Hardness-stress-strain correlation in titanium open die extrusion: an alternative to visioplasticity. *Journal of Materials Processing Technology* 95 (1-3) , pp. 185-190.

[10] Tibbetts, B.R., Wen, J.T.-Y. (1998) Extrusion process control: Mdeling, identification, and optimization. *IEEE Transactions on Control Systems Technology* 6 (2) , pp. 134-145.

[11] Tiernan, P., Hillery, M.T., Draganescu, B., Gheorghe, M. (2005) Modelling of cold extrusion with experimental verification. *Journal of Materials Processing Technology* 168 (2) , pp. 360-366.

[12] Wang, L., Zhou, J., Duszczyk, J., Katgerman, L. (2012) Friction in aluminium extrusion - Part 1: A review of friction testing techniques for aluminium extrusion. *Tribology International* 56 , pp. 89-98.

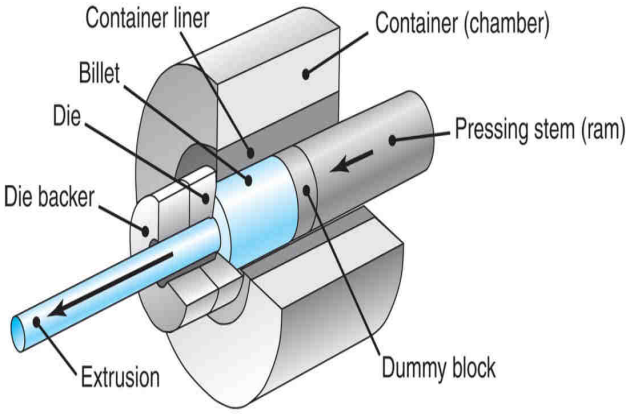

Fig. 1:Schematic of direct extrusion process.

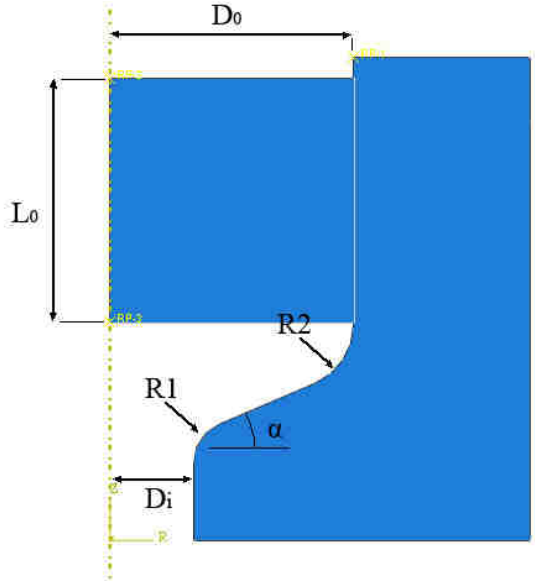

Fig.2: Important dimensions in FE model.

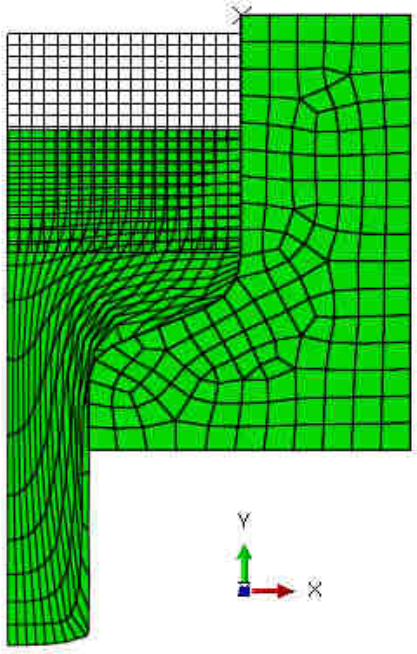

Fig.3: Undeformed and deformed FE model.

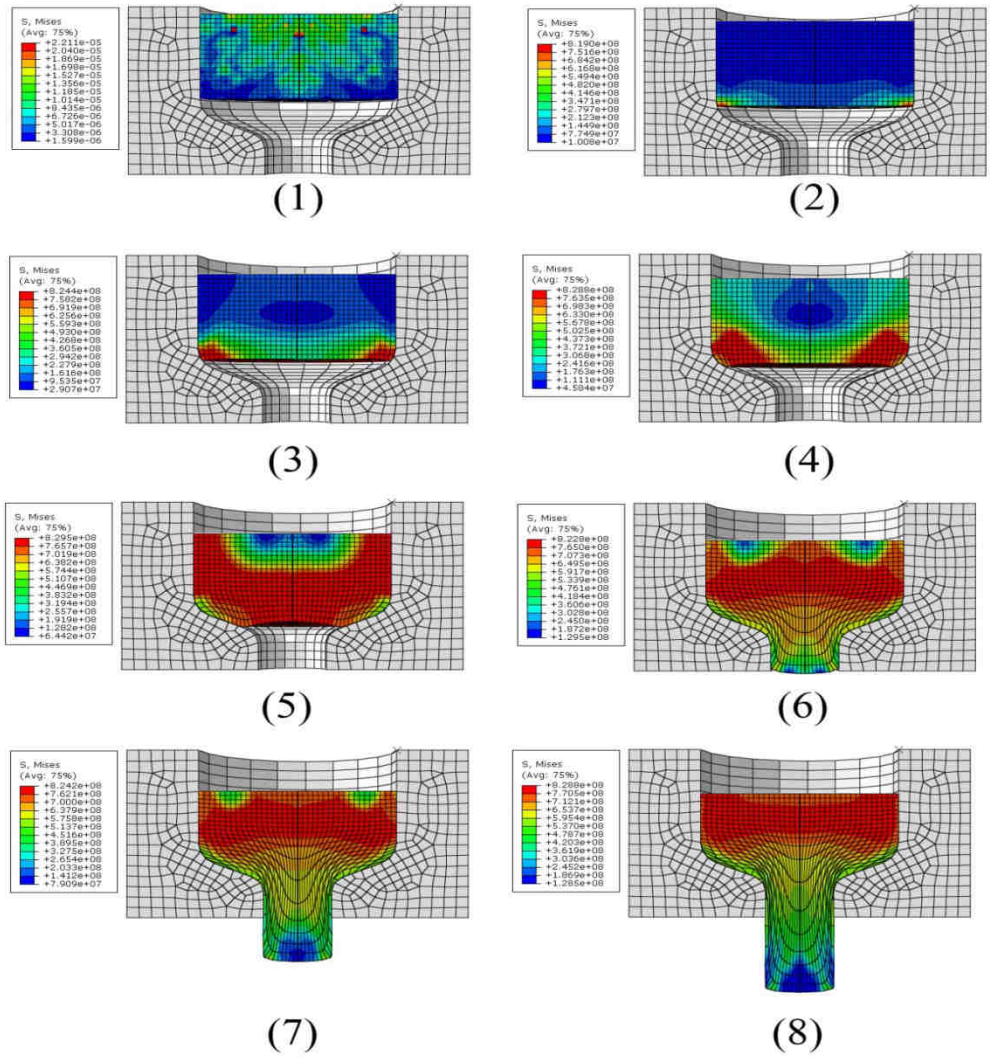

Fig.4:Development of von Mises stress in the billet in different stages of extrusion process.

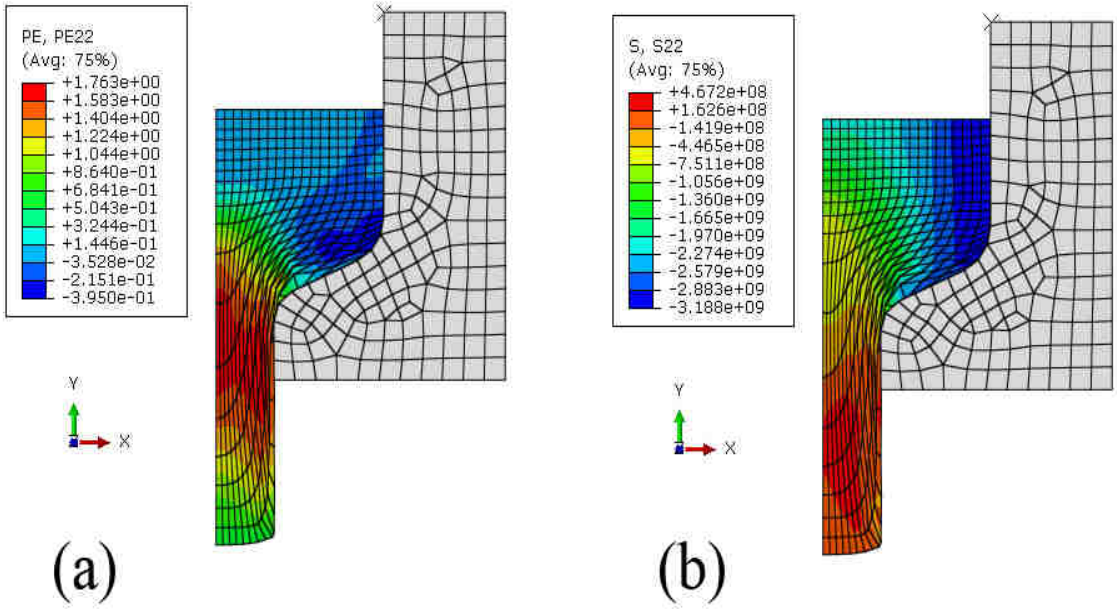

Fig.5:Distribution of (a) plastic strain, and (b) principal stress in Y direction in the last step of extrusion.

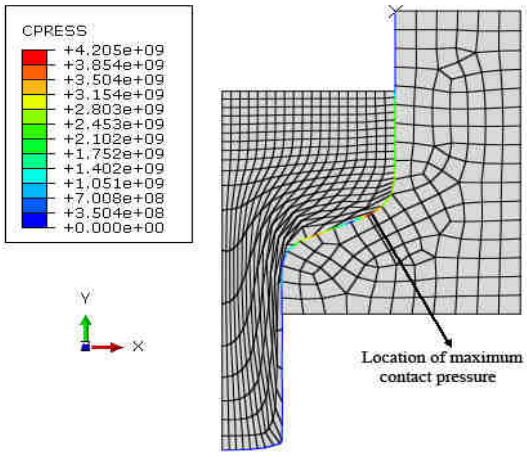

Fig.6: Distribution of contact pressure on the die surface.

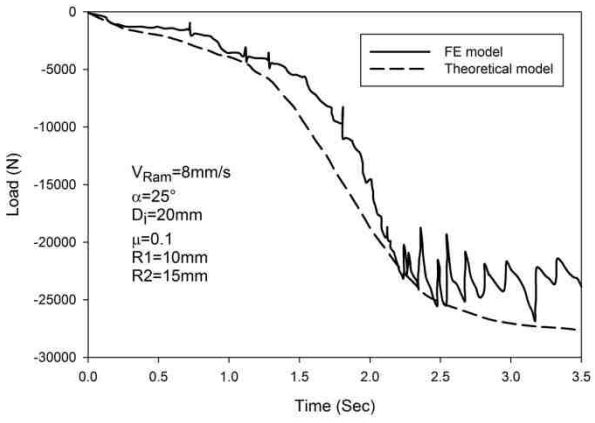

Fig.7:Comparison of theoretical and FE models ram load during extrusion process.

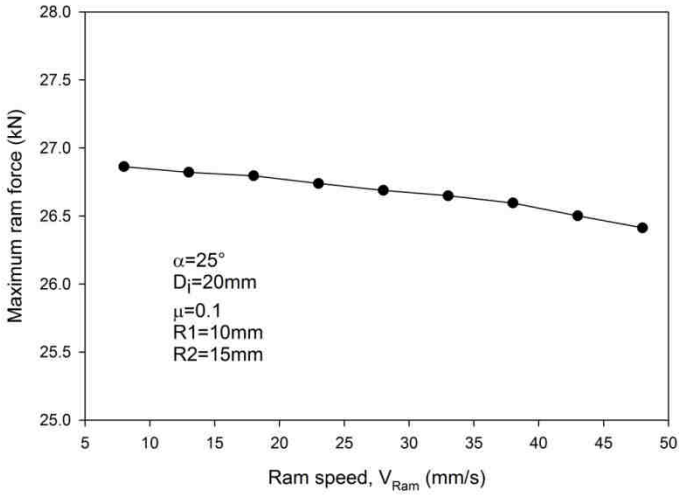

Fig.8: Effect of ram speed on maximum ram force.

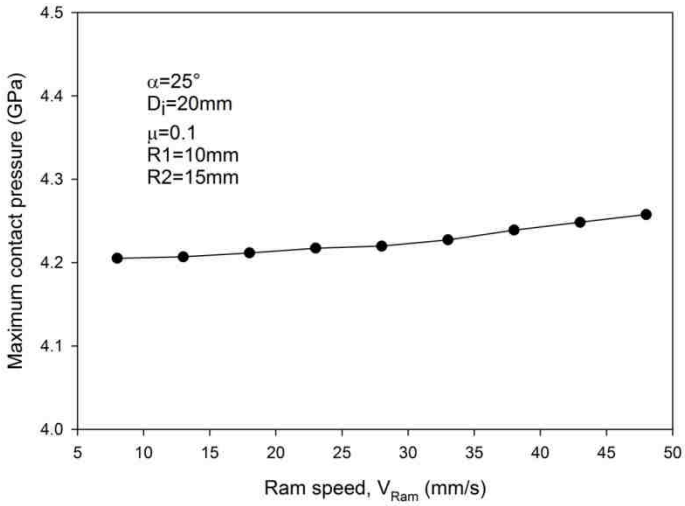

Fig.9:Effect of ram speed on maximum contact pressure on the die surface.

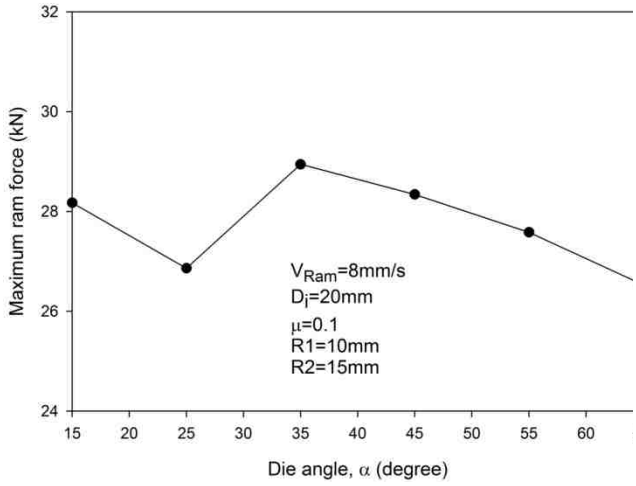

Fig.10: Effect of die angle on maximum ram force.

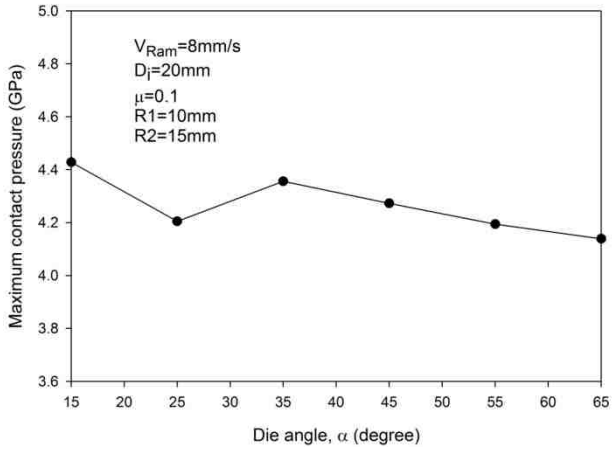

Fig.11: Effect of die angle on maximum contact pressure on the die surface.

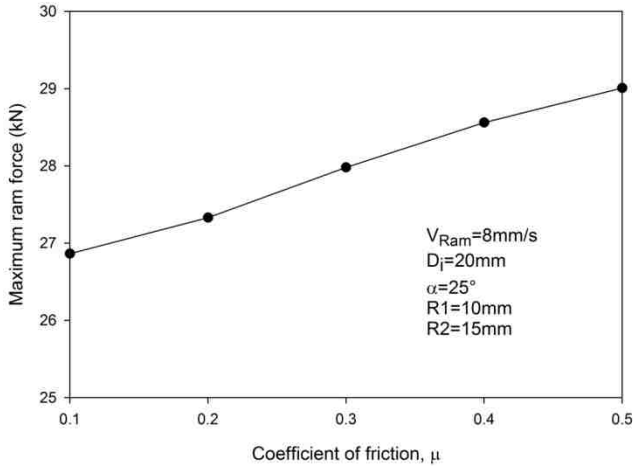

Fig.12: Effect of coefficient of friction on maximum ram force.

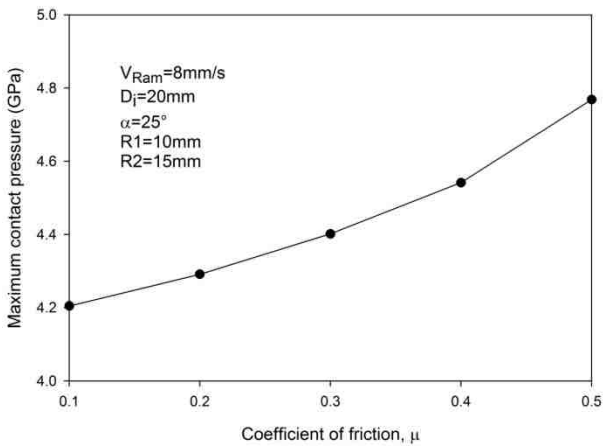

Fig.13: Effect of coefficient of friction on maximum contact pressure on the die surface.

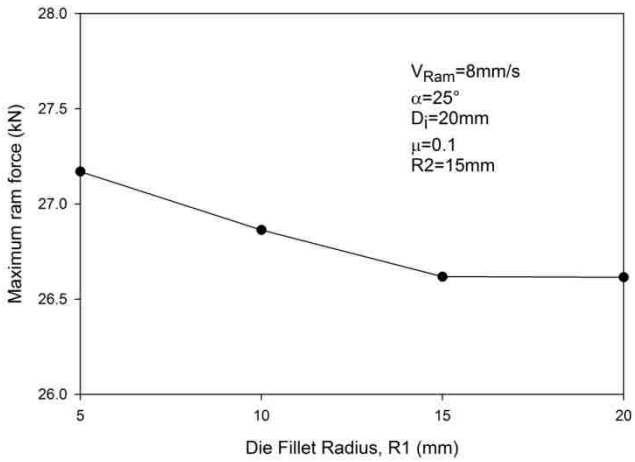

Fig.14: Effect of die angle radius on maximum ram force.

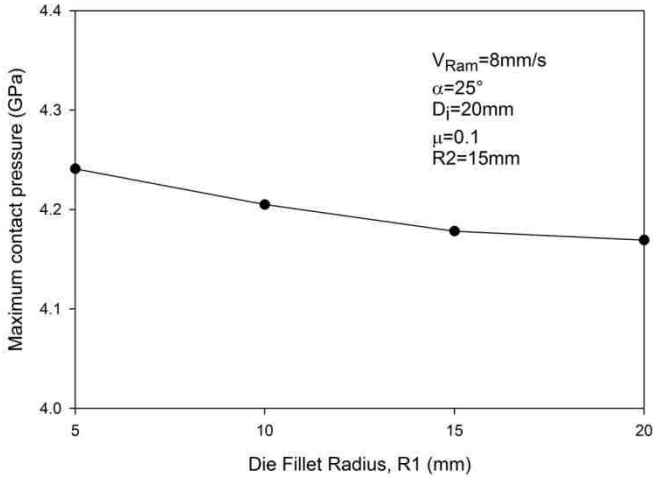

Fig.15: Effect of die angle radius on maximum contact pressure on the die surface.